Scientific African 14 (2021) e00971

Contents lists available at ScienceDirect

Scientific African

journal homepage: www.elsevier.com/locate/sciaf

Assessment of aerosol burden over Ghana ☆

Kwabena Fosu-Amankwah [a,*], Geoffrey E.Q. Bessardon [b], Emmanuel Quansah [c], Leonard K. Amekudzi [c], Babara J. Brooks [d], Richard Damoah [e]

[a] Applied Physics Department, C. K. Tedam University of Technology and Applied Sciences, Navrongo, Ghana
[b] School of Earth and Environment, University of Leeds, Leeds, LS2 9JT, UK
[c] Department of Physics, Kwame Nkrumah University of Science and Technology, Kumasi, Ghana
[d] National Centre for Atmospheric Science (NCAS), Fairbairn House, 71 - 75 Clarendon Road, Leeds, LS2 9PH, UK
[e] National Aeronautics and Space Administration/Goddard Space Flight Center (NASA/GSFC), Mail Code: 618, Greenbelt, MD 20771, Morgan State University, USA

ARTICLE INFO

Article history:
Received 4 September 2019
Revised 23 August 2021
Accepted 23 August 2021

Editor: DR B Gyampoh

Keywords:
Aerosols
AOD
Ghana
MODIS
AERONET
HYSPLIT

ABSTRACT

Although air pollution in Ghana is ranked number one in environmental health threats to public health and sixth to cause of deaths, routine monitoring is rare. This paper presents fourteen years (2005-2018) assessment of aerosol optical depth (AOD) at 3 km resolution from MODIS Aqua and Terra satellites to ascertain the Spatio-temporal and seasonal distribution of aerosols over Ghana and its major cities. The MODIS AOD at 3 km were validated against ground-based Aerosol Robotic Network (AERONET) AODs to ascertain the suitability of the MODIS 3 km data for air quality application in the region. The contribution of distant aerosols to city aerosol loadings was also assessed with Hybrid Single-Particle Lagrangian Integrated Trajectory (HYSPLIT) backscatter model. A moderate-high aerosol burden (AODs ~ 0.50) was observed over Ghana with a significant contribution from the pre-monsoon season. City centres of Takoradi and Kumasi showed higher aerosol loads (AODs ~ 0.80) than Accra and Tamale. The HYSPLIT model showed that distant or transported aerosol sources to the city centres were of both marine and land generated origins. Linear regression analysis between MODIS AOD and AERONET AOD showed a reasonably good correlation of ~ 0.60 for Aqua and Terra. From the validation analysis, both Aqua and Terra satellites can be used for air quality monitoring over Ghana; however, more ground research must be conducted to ascertain better aerosol model assumptions for the region.

Introduction

Aerosols are suspended solids, liquids or mixed-phase particles in the atmosphere with variable chemical composition and size distribution [1–3]. They originate from two main pathways: the emissions of primary particulate matter (PM) and the formation of secondary particles from gaseous precursors. Among the primary sources of aerosols are mineral dust,

☆ Editor: Gyampoh.

* Corresponding author.
E-mail address: kfosuamankwah@cktutas.edu.gh (K. Fosu-Amankwah).

https://doi.org/10.1016/j.sciaf.2021.e00971

sea salt spray, black carbon (BC) and primary biological aerosol particles (PBAPs). In contrast, sulphate, nitrate, and ammonium are secondary aerosol formation processes [4]. Both primary and secondary aerosols are influenced by natural and anthropogenic sources and can be transported thousands of kilometres by prevailing winds. The extent of the transport and distribution (vertically and horizontally) from the source is dependent on seasonal meteorological conditions. For instance, elevated aerosol layers picked up by strong winds from Africa or Asia are transported to Europe and America as observed by [5,6]. During these transportation processes, the physio-chemical properties of aerosols change via multiphase chemical transformations, cloud processing and deposition [7]. Aerosols are primarily regional due to their short lifetime, high anthropogenic contribution at regional, urban and local levels. However, the natural sources of aerosols are more significant on a global scale [8–12] compared to the anthropogenic sources.

Evidence of the diverse impact of aerosols on climate, air quality and human health has been recorded [13,14]. Directly, aerosols affect the atmospheric energy balance by scattering and absorbing radiations [15]; indirectly, they serve as cloud condensation nuclei [16] and semi-directly heat the air through absorption of radiation resulting in a reduction of low cloud cover [17]. Aerosols thus directly impact the hydrological cycle [18] and, to a more considerable extent, food security [14]. In addition to the vast impacts of aerosols on climate, human diseases such as cancer, cardiopulmonary diseases and increased morbidity and mortality, especially among infants and the aged [13,19], have also been linked to high concentrations of near-surface fine aerosols with diverse micro-organisms therein. However, the relative strength of these particles in imparting deleterious effects depends heavily on their availability and physiological properties [20]. According to [21], aerosols in the accumulation mode are of utmost importance as they can hydrate to diameters between 0.1 and 2 μm. With this feature, the accumulation mode aerosols can become very efficient in mass extinction and scattering as well as possess a greater atmospheric lifetime [22].

Many researchers have used Aerosol Optical Depth (AOD) as a proxy [e.g. [23–26]] to quantify the degree of aerosol loadings in the atmosphere. AOD is the integral extinction of columnar electromagnetic radiation due to scattering and absorption processes by atmospheric aerosols. The degree of aerosol loading is thus tied to the total column of optically effective particles, which provide more information on the available reservoir of these pollutants above each location [27]. Satellite-based AOD retrievals provide global coverage and non-intrusive measurement of Spatio-temporal examination of air quality and pollution [28]. However, these measurements are froth with errors and inaccuracies due to instrumentation, surface reflectance schemes, and retrieval algorithms [29,30]. Several studies [e.g. [26,31–35]] therefore recommend that satellite mapping and monitoring of air pollutants be related to “ground-truth” measurements such as Aerosol Robotic Network (AERONET). AERONET is a global network of ground-based sunphotometers capable of acquiring information about aerosols including columnar AODs [36].

Among the many Earth Observing Systems (EOS) in orbit, the MODerate Resolution Imaging Spectroradiometer (MODIS), consisting of the Aqua and Terra satellites, had more aerosol-related applications due to its wide swath width of 2330 km and nearly global coverage in every 1 to 2 days. Aerosol retrievals by MODIS are based on three main retrieval algorithms; Dark Target (DT) and Deep Blue (DB) algorithms over land and Dark Target (DT) algorithm over the ocean. The DT algorithm is developed for AOD retrievals over dark surfaces (dark soil and vegetation), while DB is used for AOD over bright surfaces (desert and urban regions) [37,38]. These retrieval algorithms have undergone several upgrades from collection 4 through 5 to the current collection 6.1, which provides the standard AOD retrieval at 10 km resolution, a nominal resolution at 3 km for air quality assessment on a local and urban scale. Beginning the collection 006, a new product, combined Dark Target and Deep Blue (DTB), based on the DT and DB algorithm, was also added [37]. Earlier MODIS collections have received enormous validation over many global regions than the latter. Thus, there is the need to assess the performance of this product over other geographical locations, predominantly Africa, where information on urban or local scale aerosol validation are scarce.

The present study was conducted over Ghana, a country experiencing rapid population growth and rising economic activities [39]. Due to the country’s geographical position, it experiences diverse aerosol types and loadings throughout the year. For instance, emissions from biomass burning by local farmers during land preparation periods, Saharan dust outbreaks, and the incidences of meningitis [40,41]. The speedy rise and vast redistribution of gaseous pollutants and aerosols [42] due to deep convection in the tropics, as well as the transport of Sahara dust to the Gulf of Guinea [43] through several South West African countries including Ghana [44], makes Ghana a candidate to the complex mixtures of West African aerosols. In addition, extensive economic activities in its major cities heightened by significant anthropogenic emissions from industrial activities, transportation, construction sites, petroleum extraction fields, and surface mining sites pose additional aerosol burdens on Ghana and its cities.

In spite of all these possible aerosol emission sources, routine measurements of aerosols over Ghana are scarce. Previous studies [e.g. 45] was more of a regional study than local and as such inadequate for local scale air quality assessment due to the following reasons: i) a coarse MODIS product (i.e. Level 3 gridded $1^\circ \times 1^\circ$ lower resolution) which cannot resolve aerosol at microscale, ii) “ground truth” validation of the MODIS AOD was not conducted, even though recommended due to surface reflectance challenges, complex variation of aerosols over different regions, as well as instrumentation and retrieval algorithm errors, iii) seasonal aerosol assessment which captures the contribution of local farming practices (especially during the pre-monsoon) were not considered. Besides, the study was largely based on two seasons, the dry (harmanttan) and wet seasons. However, the pre-monsoon season could have dire effect on aerosol loadings over the country as it coincides with the massive land preparation (e.g. extensive biomass burning and soil tillage) activities by local farmers in the region.

The present study therefore, seeks to provide: i) spatio-temporal aerosol assessment from MODIS 3km AOD product over Ghana; ii) validate MODIS 3km AOD product with a “ground truth” AERONET AOD data, iii) assess seasonal aerosol spatial

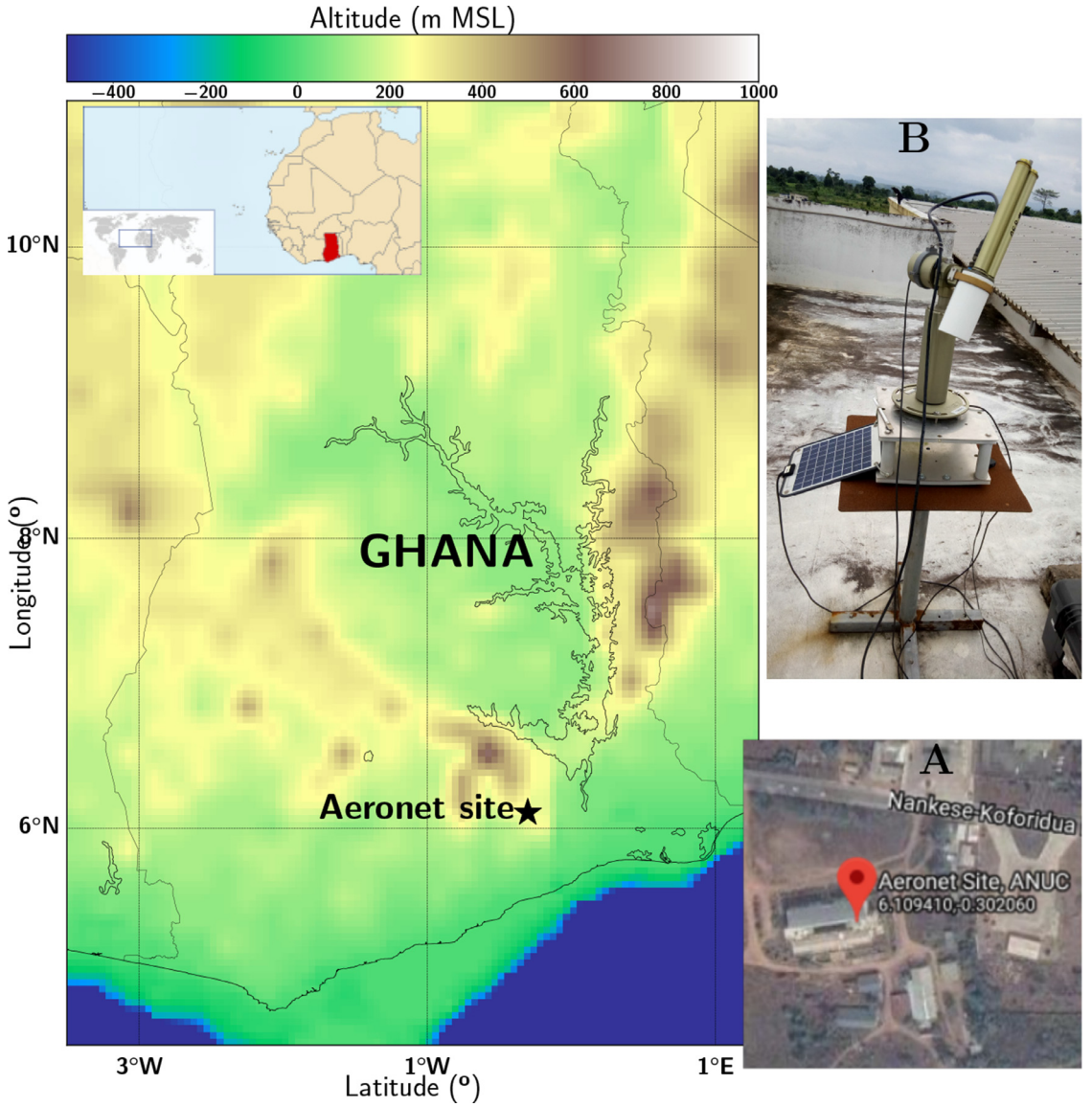

Fig. 1. A topographic (elevation measured in meter above mean sea level [m MSL]) map of Ghana with an inset (top left corner) showing the country's geographical position on the globe and the West African Region. The star (⋆) sign indicating the location of the AERONET site in the country, while inset A shows the aerial view (from google map) surrounding the AERONET site and inset B showcasing a Cimel sun-sky sunphotometer (part of AERONET) installed on top of All Nations University College (ANUC) administration block, Koforidua in the Eastern Region of Ghana.

distribution over the country, iv) ascertain inter-city aerosol variability over the country's four major cities and v) evaluate the possible contribution of distant aerosol source to city aerosol burdens. Section 2 describes the study area and prevailing meteorological conditions, datasets used and methodology. Section 3 presents the results and discussion and Section 4 the summary and conclusions.

Datasets and methodology

Study area

The study was conducted over Ghana (Fig. 1). This country lies between latitude 5° N and 11° N and longitude 4° W and 2° E and bordered by Burkina Faso to the north, Ivory Coast to the west, Togo to the east and the south by the Atlantic ocean and the Gulf of Guinea. The country has the largest man-made lake which covers an area of about 8,500 km^2 (about 4% of total area of Ghana) with an average depth of 18.8 m (∼ 62 ft) and estimated shoreline of 5,500 km [46]. The country's population is projected to be around 29.6 million (Ghana Statistical Service, GSS 2018 report) with most densely populated

region being the coastal and middle portion of the country. According to Lacombe et al. [47], about 60 % of the economically active population depend on agriculture for their livelihood. Active farming takes place during the monsoon season (as there is less irrigation farming) while land preparation and harvesting take place during the pre-monsoon and the post-monsoon seasons respectively.

The climate of Ghana is characterized by two seasons (dry and wet), a tropical monsoonal climate [48]. Rainfall in this region is mainly associated with mesoscale convective systems and is modulated by moisture flux from the Gulf of Guinea in the low-level atmosphere. The climate system is usually referred to as the West African Monsoon (WAM). It is driven mainly by the energy and temperature gradient between the Gulf of Guinea and the Sahara [49]. The Inter-Tropical Discontinuity (ITD), a region form between the continental airmass and maritime airmass, play a vital role in the WAM [50]. The annual rainfall is closely related to the north- and southward migration of the ITD, resulting in changes in the rainfall regime from the south to the country's north [48]. As a result, there are two rainfall regimes: bi-modal in the south, consisting mainly of coastal and forest zones, and uni-modal in the northern part of the country, consisting of part of the transition and savannah zones [51,52].

Annual mean rainfall over the country range from 900 to 1900 mm with the North-Western parts recording higher values compared to the Savannah and Eastern coast [52]. The onset of rains in the region begin in February while the dry or harmattan season (characterised by dry and dusty north easterly winds from the Sahara) from November to early February. Annual average relative humidity ranges from 77 % to 85 %, whereas daily mean temperatures stands at $\sim$ 30 $^{\circ}$C and $\sim$ 24 $^{\circ}$C during day and nighttime respectively [53].

Ghana has four major cities (Accra, Kumasi, Takoradi and Tamale). Accra and Takoradi are situated along the coast, whereas Kumasi and Tamale are in the middle and northern parts respectively. These cities are experiencing escalating population growth, enormous industrial and economic activities as well as high vehicular population [39]. According to [54], most vehicles imported into Ghana are over aged, undergo less maintenance and as such have high emissions.

Datasets

MODIS

MODIS consist of two sensors in orbit, one upon each of the Earth Observing System (EOS) Aqua and Terra satellites. The MODIS EOS measures reflected solar radiance and terrestrial emission in 36 channels with moderate spatial resolutions of 0.25 km, 0.5 km, and 1.0 km at an altitude of 705 km and a 55° scan view [55,56]. MODIS aerosol retrievals are based on three retrieval algorithms: Dark Target (DT) [57] and Deep Blue (DB) retrieval algorithms over land, as well as a DT retrieval algorithm over oceans [38,58]. In addition to these three main algorithms is the combined Dark Target and Deep Blue product algorithm which selects the best algorithm (i.e. DB or DT algorithm) base on land surface characteristics or type. The DT algorithms are utilised over dark surfaces such as, vegetation and dark soil and another over oceans, while the second-generation DB algorithm can be used over bright surfaces such as, deserts and urban areas as well as vegetated surfaces. Aerosol retrievals with the DT algorithm over dense vegetation and dark soil surface are based on the assumed relationship between two visible wavelengths 0.47 and 0.65 μm and one shortwave (2.12 μm) in the infra-red wavelength [55]. Aerosol properties derived from MODIS over land and ocean allow us to acquire in-depth understanding about aerosols over the globe [55].

The current operational MODIS collection, C061 provides standard aerosol parameters at a spatial resolution of 10 $\times$ 10 km^2 in the Level 2 (L2) datasets (i.e. MOD04 for Terra and MYD04 for Aqua) with lower resolution of 1° $\times$ 1° in aggregated L3 products [59]. A separate 3 km DT aerosol file is added to the C006 (presently C061) datasets for the provision of air quality information at urban or local levels. Detailed description of the C006 can be found in [60] while updates on the DT C006 which resulted in the current C061 are captured in [61]. The DT product is known to exhibit more significant uncertainty, especially when the underlying surface is bright [57]. Remer et al. [60], in validating the MODIS 3 km AOD against six months ground-based (AERONET) data, observed the same uncertainty range as the 10 km resolution (i.e. ($\pm$(0.05 + 15 %)) over land. He however, recommended that, the uncertainty range be broadened to $\pm$(0.05 + 20 %). Uncertainty for the MODIS AOD product over ocean is however maintained at $\pm$(0.03 + 5%) [58,62].

Based on the vegetation cover of the study area, that is Normalised Difference Vegetation Index (NDVI) value of approximately 60%, the DT AOD values were the best option as recommended [e.g. 37, 63].

AERONET

AERONET consist of a network of ground based remote-sensing Cimel sun-sky sunphotometers established by the National Aeronautic Space Agency, NASA to study the spatial coverage of aerosols. It estimates AODs based on Lambert-Beer-Bourguer principle - which is a direct method where spectral extinction of incident radiation at different wavelengths is measured after it has passed through the atmosphere. Errors as a result of losses due to Rayleigh scattering, ozone absorption and gaseous pollutants are corrected to obtain the optical depth above the sunphotometer. Uncertainties of the AERONET measurement lies within $\pm$ 0.02 and $\pm$ 0.01 for shorter ($<$ 440 nm) and longer ($>$ 440 nm) wavelengths respectively [36,64].

AERONET data used for the validation of the MODIS data in the present study was downloaded from https://aeronet.gsfc.nasa.gov/ web site. The AERONET site (lat:lon 6.10941 N : 0.30206 W) in Ghana is a "young" site located on the main

Table 1
Seasonal mean and average minimum and maximum AOD retrievals from Terra and Aqua over Ghana.

Season	Average Terra AOD Range	Mean Terra AOD±sd	Average Aqua AOD Range	Mean Aqua AOD ± sd
Dry	0.24 - 1.00	0.54 ±0.19	0.23 - 0.81	0.50 ± 0.15
Pre-monsoon	0.17 - 2.05	0.58 ±0.19	0.04 - 1.75	0.57 ± 0.23
Monsoon	0.20 - 1.16	0.55 ±0.19	0.11 - 0.67	0.41 ± 0.14
Post-monsoon	-0.05 - 0.96	0.48 ± 0.15	0.17 - 0.61	0.30 ± 0.08

campus of All Nations University College (ANUC), Koforidua (about 5 km away from Koforidua city centre). The Cimel sun-sky sunphotometer is installed on the roof-top (i.e. 205 metres above ground level, AGL) of the main ANUC administration block. Data collection at the site began in December 15, 2015 and still on-going. As at the time of the study, available data from the site were: Level 1.0 (unscreened) $>$ 5 years, Level 1.5 (cloud screened) $<$ 4 years and Level 2.0 (cloud screened and quality assured) $<$ 4 years. Only high quality Level 2.0 Version (V) 3.0 dataset were utilised in the present study. The V3 L2 product was used as it has some improvements, (such as removal of thin cirrus clouds which is common over the region) over the earlier version (V2) [65]. Additional site information can be found at the AERONET website (i.e. https://aeronet.gsfc.nasa.gov/).

AOD retrieval over Ghana

MODIS (Aqua and Terra) C061 L2 DT AOD product at 3 km resolution are utilised to assess spatio-temporal aerosol distribution over Ghana. The study was conducted for a period of 14 years (2005–2018). The choice to use the 3 km nominal resolution instead of the L3 gridded product previously used by [45] are based on its ability to retrieve aerosols within areas closer to coastlines (or shorelines), resolve local aerosol gradients features (such as smoke plumes) at city or urban levels and also remove cirrus clouds which frequently occur in the study area [26,30,60]. These features could be missed by the poor-resolution $1^\circ \times 1^\circ$ L3 gridded product previously utilised by [45] over the region.

Only daytime AOD dataset (wavelength, $\lambda = 0.55$ μm) at $\sim$ 10:30 am local time for Terra and $\sim$ 1:30 pm local time for Aqua overpass times were respectively downloaded from https://ladsweb.modaps.eosdis.nasa.gov/ for the study. The Scientific Data Set (SDS), Optical_Depth_Land_And_Ocean were selected for used in estimating the spatio-temporal aerosol distribution over the entire country. Data volume was increased by using all quality flagged, QF (1 - marginal, 2 - good and 3 - highest "confidence" data respectively) satellite data retrieved. The country was divided into smaller grids of $0.04^\circ \times 0.04^\circ$ (about 4×4 km^2) area and pixel fall (i.e. at least five) within these grids averaged to obtain estimated AODs for the entire country. It must be noted that no further statistical smoothening or gap filling was conducted on these dataset.

To evaluate the seasonal spatial distribution of aerosols over the country, AOD values were organised into four seasonal windows (dry/harmattan, pre-monsoon, monsoon and post-monsoon seasons) instead of the two main seasons observed in the country. This was done so as to capture the contribution of land preparation activities by local farmers (predominantly during the pre-monsoon season) to aerosol burden and distribution over the country. This was done so as to gain the true picture of MODIS Aqua and Terra AOD retrievals over the country.

AOD over selected cities in Ghana

Aerosol loadings over the four major cities in Ghana were estimated by collecting MODIS AOD data over an area of $0.02^\circ \times 0.02^\circ$ (about 2×2 km^2) longitude and latitude centred on each city centre as was done elsewhere by Gupta et al. [66]. The data was downscaled to obtain higher resolution. To assess the level of aerosol loadings over the four major cities, spatial distribution of mean AODs from city centres were obtained by drawing three different circles of radius 25 km, 50 km and 75 km centred on each city centre. The estimated means and standard deviations of AODs were then calculated using all pixel fall within each of the grid boxes in the circle. Spatial distribution of AODs from city centres to the outskirts were assessed to get the trend of aerosol loadings from the city centres to the outskirts (Table 1). All quality flags (QFs) were incorporated into the data analysis to increase data volume as in the previous section.

To ascertain the impact of distant aerosol sources on the cities aerosol burden, 7 days backward airmass trajectory during aerosol episodes (defined here as, periods with AOD$\geq$ 3.0 centered on the city centre) were assessed by using the Air Resource Laboratory's (ARM) Hybrid Single-Particle Lagrangian Integrated (HYSPLIT) backward trajectory model. The backward trajectory was performed for seven days as aerosols reside in the lower troposphere for about 7 days [67].

MODIS AOD validation with AERONET AOD data

To validate MODIS AOD data, three years (2016–2018) direct sunlight AOD measurement from AERONET L2 Version 3 (V3) are utilised. The AERONET AOD data were downloaded from http://aeronet.gsft.nasa.gov. The L2 data is used because, of its high quality assurance (QA) as it is automatically cloud screened and has undergone pre and post field calibration. For a point to be incorporated into the validation analysis, AERONET and MODIS AOD measurements were matched in space and time. This spatial matching was achieved by making grids of $0.02^\circ \times 0.02^\circ$ (about 2 km^2) within a circle of fixed radius 7.5 km around the AERONET site as prescribed by Remer et al. [60], for the validation of MODIS 3 km AOD

product. To increase the number of statistical samples for the validation, collocation was defined as the average of at least 2 AERONET AOD measurements within 1 h (± 30 min) overpass time for Aqua and Terra. Only MODIS AOD pixels with very high quality assurance (QA = 3) are averaged over the AERONET site for the sake of consistency with pre-launch validation by the MODIS DT science team [57]. For a better comparison, AERONET AODs were interpolated to match the MODIS AOD retrieval wavelength (0.55 μm), as the AERONET sunphotemeters do not retrieve AODs at 0.55 μm. In achieving this, second order polynomial fit technique (Eq. 1) utilised by Eck et al. [64] and Roy et al. [68] was applied.

$$ln(AOD) = a_o + a_1 ln\lambda + a_2 (ln\lambda)^2 \tag{1}$$

Simple linear regression model was used to establish the relationship between AOD from AERONET and the MODIS 3 km AOD product. The model was performed on the MODIS and AERONET match-up AODs to determine the slope c and intercept m between AERONET AOD (A_τ) and MODIS AOD (M_τ).

Statistical indicators such as, relative mean bias (RMB, Eq. (2)), root mean square error (RMSE, Eq. (3)), mean absolute error (MAE, Eq. (4)), correlation coefficient (R, Eq. (5)) were conducted to ascertain data quality and precision between the MODIS space borne AODs and that of the AERONET "ground truth" AODs as done elsewhere [e.g. 58, 69–72, 73]. The RMB indicate the overall bias between the MODIS and AERONET AODs. RMB > 1 depicts overestimation and RMB< 1 indicates otherwise. The correlation coefficient, R shows the consistency in data between the two instruments, higher R-value portrays better agreement, and the vice versa while a higher RMSE signifies poor agreement or otherwise. MAE, on the other hand shows the average prediction error between pair-observations in a regression model [74]. MAE < 1 shows lower prediction error and the vice versa.

As fewer than 100 collocated points were obtained for the three year period, bootstrap confidence interval technique was used to ascertain the level of uncertainty and precision between AODs from AERONET and MODIS datasets.

$$RMB = \frac{1}{N}\sqrt{\sum_{N=1}^{N}\left|\frac{AOD_{(MD)_i}}{AOD_{(AE)_i}}\right|} \tag{2}$$

$$RMSE = \sqrt{\sum_{N=1}^{N}\frac{1}{N}\left(AOD_{(MD)_i} - AOD_{(AE)_i}\right)^2} \tag{3}$$

$$MAE = \left(\frac{1}{N}\right)\sum_{i=1}^{N}\left|AOD_{(MD)_i} - AOD_{(AE)_i}\right| \tag{4}$$

$$R = \frac{\sum_{i=1}^{N}(AOD_{(MD)_i} - \overline{AOD_{(MD)_i}})(AOD_{(AE)_i} - \overline{AOD_{(AE_i}})}{\sqrt{\sum_{i=1}^{N}(AOD_{(MD)_i} - \overline{AOD_{(MD)_i}})^2 \sum_{i=1}^{N}(AOD_{(AE)_i} - \overline{AOD_{(AE)_i}})^2}} \tag{5}$$

$$EE = \pm(0.05 + 20\% \times AOD_{AE}) \tag{6}$$

AOD_{MD} and AOD_{AE} represent AOD at 0.55 μm wavelength from MODIS and AERONET respectively. EE is the 1 standard deviation estimated confidence envelope (expected error) within which the 3 km MODIS AOD is considered probable [60].

Results and discussion

Fourteen-years AOD distribution over Ghana

Figure 2 (a and b) shows the climatological outlook of aerosol burden over Ghana, and Fig. 2c, a corresponding Giovanni generated Normalised Difference Vegetation Index (NDVI) climatology for the same period of the study. The NDVI map provides information on vegetation coverage over the country as it has effect on the choice of AOD retrieval algorithm used [75]. The AOD spatial distribution map shown in Fig. 2a and b are based on AODs at 550 μm wavelength for a period of fourteen years (2005–2018) from MODIS (Aqua and Terra) retrievals. It can be observed from both maps that, MODIS successfully retrieved AODs over the entire country. Mean AOD values of 0.410 (± 0.143 standard deviation, sd) and 0.544 (± 0.187 sd) were respectively obtained for Aqua and Terra over Ghana. The Terra DT algorithm yielded greater mean AOD compared to the Aqua counterpart. The reason for this discrepancy could be attributed to the overpass times of these two satellites. For instance, humidity values in the tropics are relatively high, especially during morning hours than it is in the afternoon. Hence, there is a greater propensity of the Terra satellite encountering aerosols with high hygroscopic growth during its passage (~ 10:30 pm) than the Aqua counterpart which does its scan in the afternoon (~ 1:30 pm local time). Further more, the Terra satellite could also "pick up" high density aerosol air mass during its passage from morning "rush hour" emissions (such as, soot from wood fire, largely used for domestic and commercial food preparations in the region, exhaust fumes from over-aged vehicles, etc.) and previous nights emissions, possibly retained by the stable night time and morning atmosphere. The difference in retrieval (mean Terra AOD - mean Aqua AOD) between the two satellites is quite

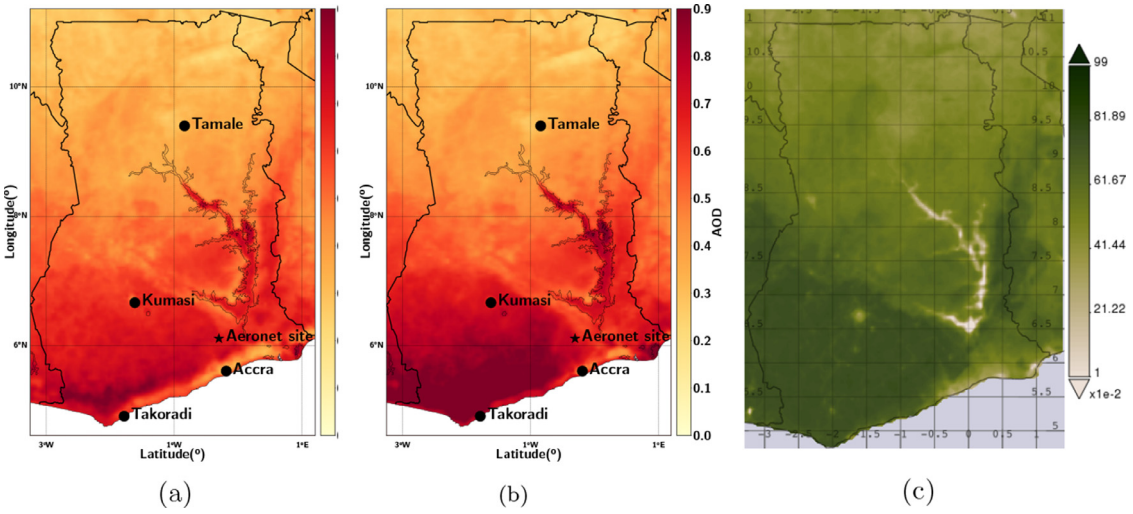

Fig. 2. Average AOD distribution over Ghana for Aqua (a) and Terra (b) retrievals and an average Normalised Difference Vegetation Index (NDVI [MODIS-Terra MOD13C2 V006]) map at 0.05 ◦ spatial resolution (c) over Ghana for the same climatological period as that of the AOD study period.

significant (0.134). The observed offset between Aqua and Terra AOD retrievals in the present study is consistent with a study by Levy et al. [76] who observed systematic difference of about 13% between Aqua and Terra AOD retrievals globally.

Overall, high AODs are observed to be concentrated around the south western parts of the country, while sparsely high AOD variations are observed at the mid and south eastern borders. The high AODs over the south western part of the country could be attributed to the fact that the DT algorithm performs well over dark surfaces such as dense vegetation and dark soils. These surface characteristics can be said about the south western part of Ghana as could be observed in the NDVI map (Fig. 2c). This part of the country covers an area of about 2,3921 km^2, approximately 10% of the total land mass of Ghana. Out of this land mass, seventy five percent (75%) of its vegetation lies within the high forest zone and the equatorial climatic zone. These high vegetation cover characterised by moderate temperature could serve as a major source of primary biogenic aerosols as it has been observed elsewhere by Charlson et al. [77]. The DT algorithm utilised in study, also does better retrievals over such areas.

Furthermore, the high AOD values observed in the south western Ghana could also be as a result of sea salt spray aloft the atmospheric column or even aerosols released from source regions, as these contribute directly to local dust loadings and thus can impact on aerosol loadings. The comparatively high AODs observed at the mid and eastern borders could be attributed to anthropogenic emissions including, fine and coarse particulate matter from surface mining activities, black carbon (BC) emissions from biomass burning and aerosols from distant origins as well as the topography of the surrounding area. The eastern corridors of the country has some range of mountains, the Akuapim - Togo mountain range. These high lands do affect aerosol dispersal and containment, and as such could be a contributing factor to the relatively high AODs observed at the eastern corridors.

Areas where low mean AODs were recorded include the northern parts of Ghana, areas along the eastern coast and some portions of the eastern region. The northern and the eastern coast have sparse vegetation and in some cases dense urban settlement (especially along the eastern coast). Such areas are characterised by bright surfaces and as such the DT algorithm may not perform very well. The low AOD values recorded could also be attributed to aerosol transport from these regions, as high or low AOD regions could be described as major sources of aerosols or receptors.

It must be made clear here, that we (the researchers) are mindful of the possible artefacts that inland waters such as the Volta lake may pose to satellite retrieval of AODs and are aware of MOD44W data for masking out such inland water bodies. In our study however, the Volta lake was not masked out due to two reasons related with the current MOD44W data, 1) the available MOD44W data were not up to date (available data is up to 2015) as it was short of 3 more years data to make-up to the duration of the present study, 2). Errors in the reprojection of the MOD44W Volta lake data were also observed as some of the points fell outside (not presented in the study) the delineated coverage areas of the lake. For these reasons the researchers rejected using MOD44W to mask out the Volta lake during the study.

The observed high AODs over the Volta lake may not be artefacts as, 1) the MODIS 3 km resolution has the ability to retrieve aerosols within coastlines (shorelines) [60]; 2) the Volta lake with an average depth of 18.8 metres (∼ 63 ft) is a shallow inland water according to depth threshold definition by the MODIS inland water (MOD44W) mask team [78]. Per this grouping and the geographical position, some of the tributaries of the Volta lake, can be ranked as ephemeral waters during prolonged dry seasons. According to Carroll et al. [78], during such periods, the "continuity of the rivers are lost as the width could be smaller than 500 m. This posses some constraints to the 500 m spatial resolution from which the MOD44W inland water masking is done. The ephemeral "behaviour" together with the long shorelines (∼ 5,500 km) of the

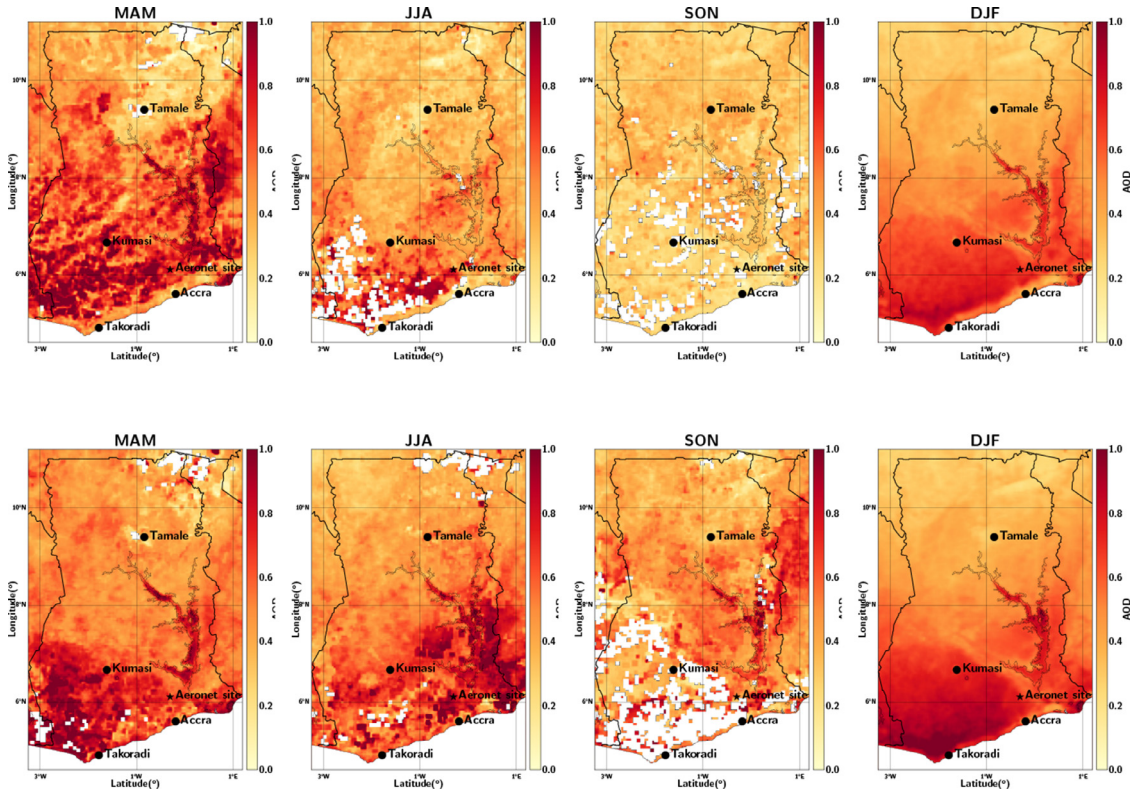

Fig. 3. Seasonal AOD trend over Ghana from both Aqua (upper panel) and Terra (lower panel) retrievals. Dry Season (December to February, DJF), Pre-monsoon (March to May, MAM), Monsoon (June to August, JJA) and Post-monsoon (September to November, SON).

Volta lake as well as surrounding biomass burning and charcoal production [79] activities could be among the causes of the high AODs observed over the Volta lake and not necessarily artefacts. In addition to the above reasons, the high AODs over the Volta lake could also be attributed to the possibility of high aerosol concentrations over the lake due to temperature inversion induced by local wind regimes from the lake or its shorelines as was observed elsewhere by Hewson and Olsson [80] (published online in March, 16 2012). Similar observation described as "basin effect" was also made by Xie and Sun [81] in a study over Wuhan, China.

Seasonal AOD trend over Ghana

The dynamic and thermodynamic properties of the atmosphere play a pivotal role in aerosol loadings and distribution at any location. The degree of aerosol burden at a particular location is dictated by the air mass and trajectories associated with the region in a given period of time [82]. Due to the disparities in meteorological parameters such as wind speed and direction, temperature and relative humidity, the seasonal trend analysis of AODs were conducted by dividing the time series into four meteorological seasons, Dry or Harmattan (December to February, DJF), Pre-monsoon (March to May, MAM), Monsoon (June to August, JJA) and Post-monsoon (September to November, SON). Among these seasons, the dry and monsoon periods are the two contrasting seasons, while pre-monsoon and post-monsoon are transition seasons.

Figure 3 shows the seasonal climatological AOD maps for Aqua (upper panel) and Terra (lower panel) over Ghana with corresponding values displayed in Table 1. It can be observed here that, similar seasonal AOD patterns were observed by both Aqua and Terra during the pre and post monsoon season. Maximum average AODs and highest seasonal mean AODs from both Aqua (1.75 and 0.57) and Terra (2.05 and 0.58) satellites were all recorded in the pre-monsoon season. Similarly, both Aqua (0.61 and 0.30) and Terra (0.96 and 0.48) recorded their least average maximum AOD and lowest mean AOD values in the post-monsoon. This makes the pre-monsoon season a major contributor to aerosol burden in Ghana. The cause of these high aerosol loadings could be attributed to the massive land preparation activities by local farmers awaiting the onset of rains. Farming practices undertaken by these local farmers involve, slashing, extensive bush burning and land tilling which result in the release of large amount of both fine (BCs, OCs, NO_x, etc.) and coarse mode (dust, plant debris, flying ash, etc) aerosols into the atmosphere, subsequently causing a rise in AOD values during the pre-monsoon season. Long-range aerosol transport from agricultural crop residue burning from neighbouring countries due to the redistribution of gaseous pollutants and aerosols [43] and the passage of the north-east trade winds [42] can also add up to the high mean AODs

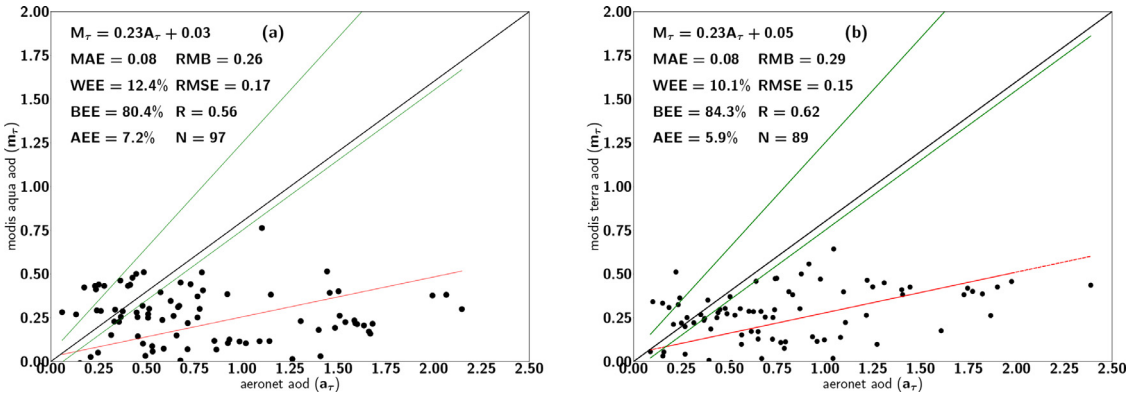

Fig. 4. MODIS AOD vs AERONET AOD inter-comparison for Aqua (a) and Terra (b). Root Mean Square Error (RMSE), relative mean bias (RMB), coefficient of correlation (R) and number of matched-up point (N). The red, black and green solid lines represent linear regression fitting line, 1:1 line and upper and lower expected error envelope respectively. (For interpretation of the references to colour in this figure legend, the reader is referred to the web version of this article.)

observed in the pre-monsoon season. According to [83], in a study elsewhere, air contaminated by aerosols from biomass burning can contribute four times the total number of particles recorded in uncontaminated air.

While similar seasonal AOD patterns were observed by both Aqua and Terra satellites in the pre and post-monsoon seasons, the two contrasting seasons (i.e. dry and monsoon seasons) witnessed significant seasonal variation in AOD retrieval patterns. Terra recorded its second highest mean and average maximum AODs in the monsoon season, whereas Aqua recorded its second highest and maximum average AODs in the dry season. The least average minimum AODs were expected in the monsoon season due to aerosol scavenging by rains, however these values were recorded by Terra (-0.05) in the post-monsoon season while Aqua (0.04) recorded its average minimum in the pre-monsoon season. These two transitional seasons are characterised by intermittent rains which may cause a " wash-out" of aerosols hence the least values. The highest average minimum AOD ~ 0.24 were recorded by both satellites in the dry season. This outcome can be attributed to the continuous passage of dry and dusty air mass from the Sahara desert through SWA including Ghana to the Gulf of Guinea at all times during the dry season. Both Aqua and Terra satellite may sample similar air masses hence recording almost same average minimum AOD value (see Table 1.).

The strong disparities in the seasonal AOD retrievals observed by both Aqua and Terra satellites could be attributed to the satellites sampling different air masses during their overpass times. In the morning hours, local aerosol emissions and residual pollutants of the previous nights may dominate due to static stability of the morning boundary layer compared to the afternoons where there is significant atmospheric mixing due to convection. In such situations high AODs are possibly to be recorded by the Terra satellites compared to that of Aqua. Generally, Terra recorded high mean AODs throughout the seasons than the Aqua counterpart (Table 1).

From Fig. 3, it can be observed that, with the exception of the dry season (where "rainy" clouds hardly form), all the maps for the other seasons have some white patches. These white patches are places where the MODIS DT retrieval algorithm "breaks down". The "near" impossible or no retrieval situation observed especially over the western sections of Ghana during the monsoon and post-monsoon seasons can be attributed to the presence of low stratiform clouds which frequently form over the SWA region (i.e. from Ivory Coast through Ghana to Nigeria and up to a latitude of 9°) [84,85]. According to Remer et al. [60], the DT algorithm avoids clouds and as such AOD retrievals are not be performed under these cloudy conditions. It must however be noted that, this does not mean the absence of aerosols below the clouds.

Validation of MODIS with AERONET

To ascertain the validity of the satellite AOD output, "ground truth" AERONET AOD data are compared with the space borne MODIS (Aqua and Terra) AOD data. Figure 4(a and b) presents the validation and statistics related to the degree of accuracy between AOD retrievals from MODIS space borne system and the ground based sunphotometer (AERONET). Figure 4a, shows AOD retrieval comparison between MODIS Aqua and AERONET while Fig. 4b, provides the comparison between AERONET and MODIS Terra. From each figure are statistical measures such as root mean square error (RMSE), relative mean bias (RMB) and mean absolute error (MAE), 1:1 line and expected error (confidence interval, CI). Relationship between the MODIS and AERONET datasets are assessed by a simple linear regression line while the strength of the linear relationship are ascertained from the correlation coefficient (R) between the number of match-up points (N). Match-up points were obtained from a three year (2016 - 2018) MODIS - AERONET dataset. More match-up points were obtained between AERONET-Aqua (A-A) (N = 97) than AERONET-Terra (A-T) (N = 89).

The disparity in the match-up points observed between A-A and A-T could be attributed to the possible encounter of more thin cirrus clouds (common within the region especially, during morning hours) during Terra overpass time than may

Table 2
Geographical position and average AOD values ± standard deviation over the four major cities of Ghana. Only MODIS Terra AOD values were considered (2005–2018).

Variables	Accra	Tamale	Takoradi	Kumasi
Latitude	- 0.1870	- 0.8393	- 1.7831	- 1.6163
Longitude	5.6037	9.4007	4.9016	6.6666
AOD (25 km radius)	0.64 ± 0.09	0.33 ± 0.03	0.82 ± 0.13	0.82 ± 0.14
AOD (50 km radius)	0.70 ± 0.07	0.36 ± 0.03	0.83 ± 0.16	0.70 ± 0.07
AOD (75 km radius)	0.71 ± 0.10	0.38 ± 0.03	0.84 ± 0.14	0.68 ± 0.07

possibly occur during the Aqua overpass time. According to Huang et al. [86], the presence of such clouds can introduce on the average 25% contamination in AOD retrievals hence are rejected by the V3 AERONET algorithm [65] which is utilised in the present study. This, together with the use of only high quality assured (QA) data from MODIS could be the major reason for the reduction in the number of match-ups points between A-T. The extra cirrus clouds present in the MODIS AOD retrievals are of degraded quality assured confidence (QAC) [37] and hence not used in the current validation study. The observation made in the current study is in disagreement with a number of observations elsewhere [e.g. [26,87,88]] where, more match-ups were observed between A-A than there was between A-T.

From both Aqua (Fig. 4a) and Terra (Fig. 4b), it could be observed that, a small fraction of only 12.4% and 10.1% respectively of the data, fall within the EE of the MODIS DT 3 km AOD algorithm. The observed high percentage of points below the expected error, BEE = 80.4%, 84.3% for both Aqua and Terra with corresponding lower RMB values of 0.26, 0.29 show overall underestimation by both Aqua and Terra DT algorithm over the study area. Overestimation of AODs by both Aqua and Terra were however on the low, as small percentage $\sim < 8\%$ of match-up points were above the EE.

Fairly strong linear relationship exist between A-A and A-T AODs as R-value of 0.56 and 0.62 were found between A-A and A-T respectively. The near zero (~ 0.08) MAE for both A-A and A-T and the lower RMB (Aqua, Terra: 0.26, 0.29) show there is relatively smaller bias between the space borne MODIS derived AODs and the ground-based AERONET measured AODs. The outcome from the comparison shows that both Aqua and Terra satellites can be used for air quality purposes locally as most of the statistical uncertainty tests show good precision. However, attention must be paid to the assumption of the aerosol model used as the slope of the linear relationship is far less than 1.

AOD estimated from city centres

Spatial distribution of aerosols loadings over the four major cities in Ghana are presented in Fig. 5 with the city center location indicated with a star ($\star$) sign. Shown in Table 2 are also the summary of the mean spatial AODs (from Terra) together with their standard deviations ($\pm$ sd) at a radius of 25, 50 and 75 km centred on each city center. The Terra satellite was used for the spatial inter-city aerosol distribution assessment as the Terra satellite showed better linear relationship in the validation assessment than the Aqua counterpart. Takoradi was observed to have the highest aerosol loadings with AOD values ranging from 0.82 (25 km radius) to 0.84 (at 75 km radius). This makes Takoradi the most aerosol burdened city in Ghana, with most of its aerosol loadings concentrated outside the city centre. Kumasi, however has the highest mean AOD (0.82) within the 25 km radius, making its city center the most polluted. The mean AOD value observed in Kumasi city centre is however the same as that observed in Takoradi city centre. Aerosol burdens in Kumasi however, decreases (0.82 to 0.64) as one moves to the outskirts of the city. The highest AOD value recorded over Takoradi (in 50 and 75 km radius) could be as a result of emissions from industrial sites which are mostly sited away from the city centre as well as contributions from sea salt spray and emissions from offshore oil and gas industries based on prevailing wind speed and direction due to the city's proximity to the coast.

Aerosol loadings over Accra saw an increasing trend from the city centre to the outskirts (0.64 to 0.71). Among the four major cities assessed, Tamale recorded the least aerosol loadings with mean AOD value of 0.33 from the city center to 0.38 along the outskirts. The high aerosol loadings observed in the city centre's (25 km radius) of Takoradi and Kumasi could be attributed to similar town planning or design as most commercial activities are centred within the city centre. In such a situation, high anthropogenic activities especially, that due to vehicular emissions as a result of dense traffic congestion could result in high aerosol loadings as observed whiles the low AODs recorded over Accra and Tamale could be attributed to "less centred" town planning approach as well as similarities in surface characteristics. Accra and Tamale have similar vegetation and soil type (coastal savanna/savanna and sandy soil) which are described as bright or urban surface per the DT algorithm and as such AOD retrievals could be poor.

HYSPLIT Trajectory Model

The impact of distant aerosols on aerosol loadings in the cities, are assessed by running the HYSPLIT model [89] using the NCAR/NCEP reanalysis data at 1° resolution with the isentropic vertical velocity procedure to ascertain air-mass origin to the four major cities of the country. The HYSPLIT model was performed during aerosol episodes. Aerosol episodes were defined as periods with AODs ≥ 3.0 over each city centre during the 14 years study period. As aerosols have short life time in the

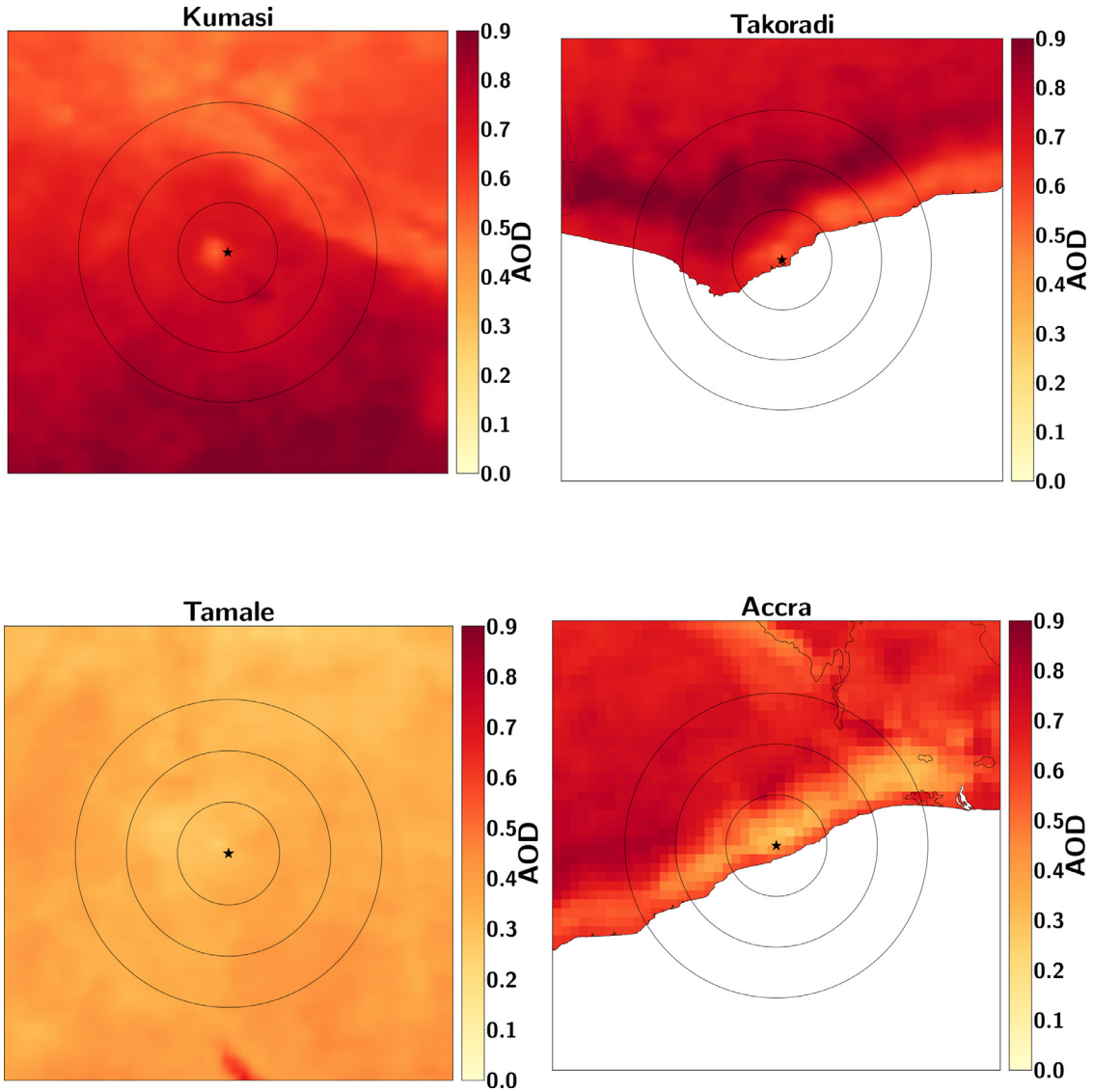

Fig. 5. Spatial distribution of AODs over the four major cities (Kumasi, Takoradi, Tamale and Accra) in Ghana. The star (⋆) sign indicate the city centre and circles of 25, 50 and 75 km radius drawn round the city centre.

atmosphere, seven (7) days backward trajectory was run over all the cities. Aerosol episodes were not recorded in any of the cities studied with the exception of Kumasi which recorded five events (i.e. 04/03/2007, 21/02/2008, 22/02/2008, 24/03/2010 and 14/04/2015). Distant air-masses were centred on each city's centre by considering air-masses at three different altitudes (250, 500 and 750 mAGL) as displayed in Fig. 6.

From Fig. 6, distant aerosols to Kumasi are of both marine and inland sources. Distant air-masses which could transport aerosols to Kumasi are observed to be originating from Nigeria at altitudes above 750 mAGL. All other air-masses probably carrying distant aerosols to Kumasi during aerosols episodes are of marine origin. Air-masses from the Gulf of Guinea and the Atlantic ocean could contain aerosols such as sea salt spray [90,91] is considered as a major primary constituent of marine aerosols, VOCs, dimethyl sulphate (DMS) aliphatic amines, DMS, aliphatic amines, monoterpenes and isoprene which is capable of forming SOAs [92]. Theses marine air-masses may also carry aerosol aerosols released into the atmosphere by gas flare from the off-shore petrochemical industries of the coast of Ghana.

Per the model outcome, locally generated aerosols could be a major contributor to the high aerosol loadings observed in the cities studied.

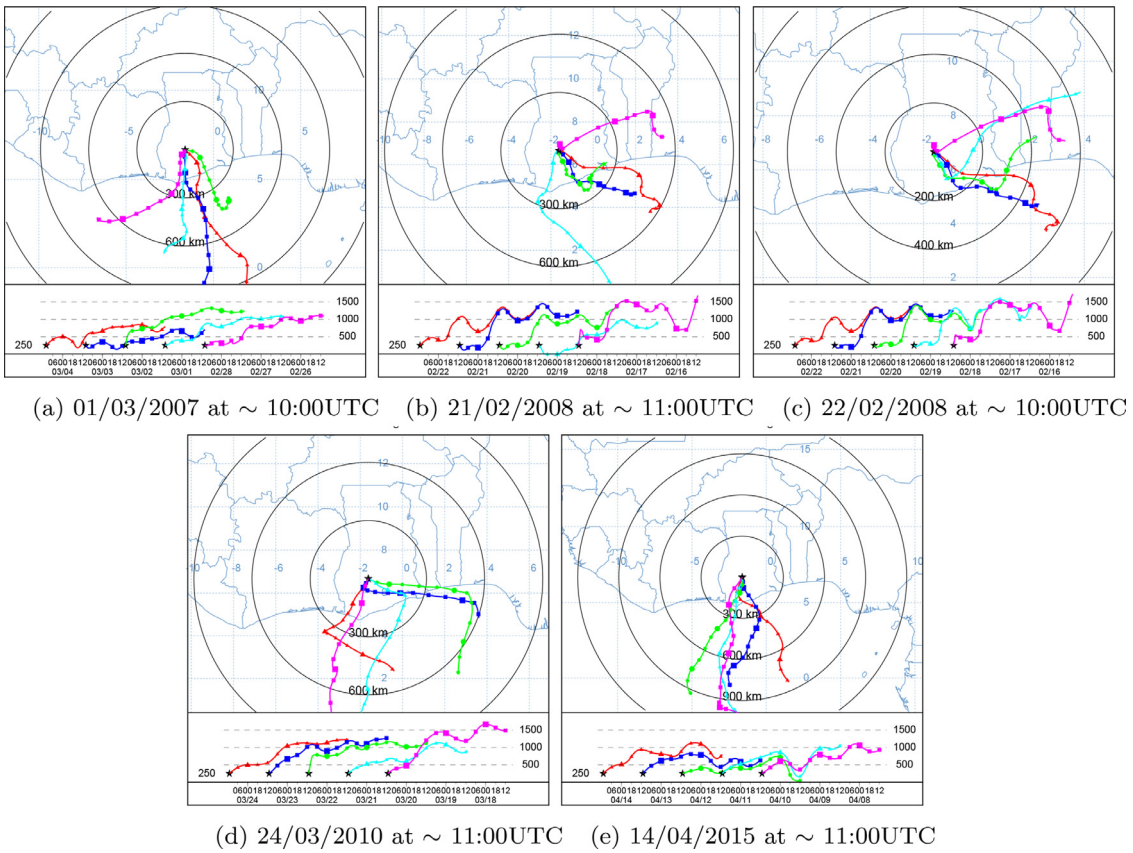

(a) 01/03/2007 at ∼ 10:00UTC (b) 21/02/2008 at ∼ 11:00UTC (c) 22/02/2008 at ∼ 10:00UTC

(d) 24/03/2010 at ∼ 11:00UTC (e) 14/04/2015 at ∼ 11:00UTC

Fig. 6. A 7-day HYSPLIT backward trajectory model of aerosol source origin during aerosol episodes (AOD ≥ 3.0) over Kumasi during the 14 years study period. Fig. 6(a, b, c, d and e) represent different aerosol episode days. The red, blue, green, cyan and pink lines represent airmass at different altitudes (i.e. 250, 500, 750, 1000 and 1500 mAGL) arriving at the city centre of Kumasi on different days. (For interpretation of the references to colour in this figure legend, the reader is referred to the web version of this article.)

Conclusions

The study presents a fourteen year (2005–2018) spatio-temporal and seasonal aerosol distribution assessment over Ghana and its major cities by utilising MODIS AOD at 3 km resolution. Distant aerosol source origins to the cities were performed by using the HYSPLIT backward trajectory model. In order to ascertain the reliability of the MODIS AOD at 3 km resolution for air quality at a local gradient, the MODIS AOD data were validated against a three-year ground-based version 3 (V3) AERONET AOD data.

The spatio-temporal aerosol distribution from MODIS Aqua and Terra AOD retrievals showed that Ghana has a lower aerosol burden as mean AODs from the two satellites were ∼ 0.5. Retrieval patterns from the two satellites were consistent with a 0.134 difference between mean Terra and Aqua AODs. By visual inspection, the southwestern part of the country showed higher aerosol loadings, and the northern and the eastern coast showed low loadings. The higher aerosol loadings observed over the south western parts of Ghana could be attributed to its dense vegetation coverage and the possible higher biogenic emissions. The DT algorithm also performs better over dark surfaces such as dense vegetation, impacting the higher aerosol observation. Deposition of sea salt spray due to a bubble bursting from the ocean and emissions from oil and gas industries off the coast of western Ghana could also add to the higher aerosol loadings over southwestern Ghana due to its proximity. The other parts of the country where lower loadings were observed are either urban or savannah areas with many bright surfaces and might be the reason for the lower AODs.

During the study, strong seasonal aerosol distribution patterns were observed, with significant contributions from the pre-monsoon (MAM) season (mean AODs ∼ 0.6). The higher aerosol loadings observed in the pre-monsoon season could be attributed to land preparation activities by local farmers awaiting the onset of rains in the monsoon. These activities are characterised by intense biomass burning and soil tillage with the possible release of large amounts of aerosols or PMs into the atmosphere. The least seasonal mean (AOD ∼ 0.4) was observed in the post-monsoon season. This observation could be a result of excess scavenging due to intermittent rains in the post-monsoon seasons. Extreme aerosol loading disparity was observed between the two contrasting seasons, dry/harmattan and monsoon season, attributable to the meteorological

changes. In the dry season, dust transport from the Sahara is dominant in the atmosphere compared to the monsoon season, where high emissions of biogenic aerosols and particles with more remarkable hygroscopic growth may be observed.

Linear regression analysis between MODIS AOD at 3 km and AERONET interpolated AOD at 550 nm wavelength showed quite a good correlation, R $\sim$ 0.60 for Aqua and Terra. Underestimation of AODs by both satellites was observed with RMB $\sim$ 0.2, expected error and EE $\sim$ 10%. However, the level of uncertainty between AEROENT and MODIS AODs was good with MAE $\sim$ 0.08 and a near-zero intercept. The observed underestimation of the MODIS DT AOD C061 L2 product at 3 km resolution shows some uncertainties in assumptions adopted for the aerosol model used over the region. Therefore, more ground-based studies must be conducted over the region to gain more insight input to improve the assumptions adopted for the aerosol model.

Spatial inter-city aerosol distribution analysis conducted during aerosol episodes (AOD $\geq$ 3.0) for the fourteen years indicate aerosol pattern descending in the order: Takoradi, Kumasi, Accra, Tamale. It was observed that, with the exception of Kumasi, all the other three cities have aerosol loadings increasing towards the outskirts of the city centre.

Model output from HYSPLIT backscatter trajectory showed that, aside from locally generated aerosol contributions, distant aerosol sources (both land and marine generated) also contribute to city aerosol loadings.

In conclusion, Ghana is moderately polluted and to routinely monitor air quality in our cities and the country as a whole, the AOD product at 3 km resolution from the two satellites (Aqua and Terra) on MODIS Earth Observing System (EOS) can be utilised. It is however recommended that, further researches be conducted to ascertain the contribution of biogenic aerosol emissions from the dense vegetation in the western parts of Ghana and cities so as to characterise locally generated aerosols over the country.

CREDIT author statement

Conceptualization, data curation and formal analysis of the study were performed by Kwabena Fosu-Amankwah and Geoffrey E. Q Bessardon under the suppervision of Emmanuel Quansah, Leonard K. Amekudzi, Babara J. Brooks and Richard Damoah. Writng of the original draft together with the review and editing were performed by Kwabena Fosu-Amankwah with contributions from all co-authors.

Declaration of Competing Interest

The authors declare that they have no known competing financial interests or personal relationships that could have appeared to influence the work reported in this paper.

Acknowledgements

We would like to show our sincere gratitude to the NASA MODIS and Ladsweb data archive team for making available the space-borne AOD product data. We are as well grateful to the ANUC site support team and the NASA AERONET team for the production of the ground-based AOD data which is readily available for download from the AERONET data server. We are also grateful to the reviewer and the editor for their insightful comments and recommendations.

References

[1] K.Y. Kondratyev, L.S. Ivlev, V.F. Krapivin, C.A. Varostos, Atmospheric Aerosol Properties: Formation, Processes and Impacts, Springer Science & Business Media, 2006.
[2] J.-P. Putaud, R. Van Dingenen, A. Alastuey, H. Bauer, W. Birmili, J. Cyrys, H. Flentje, S. Fuzzi, R. Gehrig, H.-C. Hansson, et al., A European aerosol phenomenology–3: physical and chemical characteristics of particulate matter from 60 rural, urban, and kerbside sites across Europe, Atmos. Environ. 44 (10) (2010) 1308–1320.
[3] W.C. Hinds, Aerosol Technology: Properties, Behavior, and Measurement of Airborne Particles, John Wiley & Sons, 2012.
[4] O. Boucher, D. Randall, P. Artaxo, C. Bretherton, G. Feingold, P. Forster, V.-M. Kerminen, Y. Kondo, H. Liao, U. Lohmann, et al., Clouds and aerosols, in: Climate Change 2013: The Physical Science Basis. Contribution of Working Group I to the Fifth Assessment Report of the Intergovernmental Panel on Climate Change, Cambridge University Press, 2013, pp. 571–657.
[5] A.D. Clarke, R.J. Charlson, Radiative properties of the background aerosol: absorption component of extinction, Science 229 (4710) (1985) 263–265.
[6] J.M. Prospero, R.T. Nees, Impact of the North African drought and El Nino on mineral dust in the barbados trade winds, Nature 320 (6064) (1986) 735.
[7] M.A. Rodriguez, D. Dabdub, IMAGES-SCAPE2: a modeling study of size-and chemically resolved aerosol thermodynamics in a global chemical transport model, J. Geophys. Res. 109 (D2) (2004).
[8] J.A. Coakley Jr., R.D. Cess, F.B. Yurevich, The effect of tropospheric aerosols on the Earth's radiation budget: a parameterization for climate models, J. Atmos. Sci. 40 (1) (1983) 116–138.
[9] Y.J. Kaufman, R.S. Fraser, Light extinction by aerosols during summer air pollution, J. Clim. Appl. Meteorol. 22 (10) (1983) 1694–1706.
[10] J.A. Coakley Jr., R.D. Cess, Response of the NCAR community climate model to the radiative forcing by the naturally occurring tropospheric aerosol, J. Atmos. Sci. 42 (16) (1985) 1677–1692.
[11] S.K. Satheesh, K.K. Moorthy, Radiative effects of natural aerosols: a review, Atmos. Environ. 39 (11) (2005) 2089–2110.
[12] M. Khoshsima, A.A. Bidokhti, F. Ahmadi-Givi, Variations of aerosol optical depth and angstrom parameters at a suburban location in iran during 2009–2010, J. Earth Syst. Sci. 123 (1) (2014) 187–199.
[13] J. Lepeule, F. Laden, D. Dockery, J. Schwartz, Chronic exposure to fine particles and mortality: an extended follow-up of the harvard six cities study from 1974 to 2009, Environ. Health Perspect. 120 (7) (2012) 965.
[14] A.K. Misra, Climate change and challenges of water and food security, Int. J. Sustain. Built Environ. 3 (1) (2014) 153–165.
[15] H. Yu, Y.J. Kaufman, M. Chin, G. Feingold, L.A. Remer, T.L. Anderson, Y. Balkanski, N. Bellouin, O. Boucher, S. Christopher, et al., A review of measurement-based assessments of the aerosol direct radiative effect and forcing, Atmos. Chem. Phys. 6 (3) (2006) 613–666.

[16] U. Lohmann, J. Feichter, Global indirect aerosol effects: a review, Atmos. Chem. Phys. 5 (3) (2005) 715–737.
[17] B.T. Johnson, K.P. Shine, P.M. Forster, The semi-direct aerosol effect: impact of absorbing aerosols on marine stratocumulus, Q. J. R. Meteorolog. Soc. 130 (599) (2004) 1407–1422.
[18] J.M. Creamean, K.J. Suski, D. Rosenfeld, A. Cazorla, P.J. DeMott, R.C. Sullivan, A.B. White, F.M. Ralph, P. Minnis, J.M. Comstock, et al., Dust and biological aerosols from the sahara and asia influence precipitation in the western US, Science 339 (6127) (2013) 1572–1578.
[19] J.F. Gent, P. Koutrakis, K. Belanger, E. Triche, T.R. Holford, M.B. Bracken, B.P. Leaderer, Symptoms and medication use in children with asthma and traffic-related sources of fine particle pollution, Environ. Health Perspect. 117 (7) (2009) 1168.
[20] E. Crosbie, A. Sorooshian, N.A. Monfared, T. Shingler, O. Esmaili, A multi-year aerosol characterization for the greater tehran area using satellite, surface, and modeling data, Atmosphere 5 (2) (2014) 178–197.
[21] J. Schwartz, D.W. Dockery, L.M. Neas, Is daily mortality associated specifically with fine particles? J. Air Waste Manage. Assoc. 46 (10) (1996) 927–939.
[22] J.T. Houghton, J.P. Bruce, H. Lee, B.A. Callander, E.F. Haites, et al., Climate Change 1994: Radiative Forcing of Climate Change and an Evaluation of the IPCC 1992 IS92 Emission Scenarios, Cambridge University Press, 1995.
[23] Y. Wu, M. de Graaf, M. Menenti, Improved MODIS dark target aerosol optical depth algorithm over land: angular effect correction, Atmos. Meas. Tech. 9 (11) (2016) 5575.
[24] A. Mhawish, T. Banerjee, D.M. Broday, A. Misra, S.N. Tripathi, Evaluation of MODIS collection 6 aerosol retrieval algorithms over indo-gangetic plain: implications of aerosols types and mass loading, Remote Sens. Environ. 201 (2017) 297–313.
[25] X. Shen, M. Bilal, Z. Qiu, D. Sun, S. Wang, W. Zhu, Validation of MODIS C6 dark target aerosol products at 3 km and 10 km spatial resolutions over the China Seas and the Eastern Indian Ocean, Remote Sens. 10 (4) (2018) 573.
[26] J. Wei, Y. Peng, J. Guo, L. Sun, Performance of MODIS collection 6.1 level 3 aerosol products in spatial-temporal variations over land, Atmos. Environ. (2019).
[27] A. Dandou, E. Bosioli, M. Tombrou, N. Sifakis, D. Paronis, N. Soulakellis, D. Sarigiannis, The importance of mixing height in characterising pollution levels from aerosol optical thickness derived by satellite, Water Air Soil Pollut. Focus 2 (5–6) (2002) 17–28.
[28] Z. Li, D.P. Roy, H.K. Zhang, E.F. Vermote, H. Huang, Evaluation of landsat-8 and sentinel-2a aerosol optical depth retrievals across chinese cities and implications for medium spatial resolution urban aerosol monitoring, Remote Sens. 11 (2) (2019) 122.
[29] J. Li, B.E. Carlson, A.A. Lacis, Application of spectral analysis techniques in the intercomparison of aerosol data. Part II: using maximum covariance analysis to effectively compare spatiotemporal variability of satellite and AERONET measured aerosol optical depth, J. Geophys. Res. Atmos. 119 (1) (2014) 153–166.
[30] P. Gupta, R.C. Levy, S. Mattoo, L.A. Remer, L.A. Munchak, A surface reflectance scheme for retrieving aerosol optical depth over urban surfaces in MODIS dark target retrieval algorithm, Atmos. Meas. Tech. 9 (7) (2016) 3293–3308.
[31] K. Badarinath, S.K. Kharol, A.R. Sharma, V.K. Prasad, Analysis of aerosol and carbon monoxide characteristics over arabian sea during crop residue burning period in the indo-gangetic plains using multi-satellite remote sensing datasets, J. Atmos. Sol. Terr. Phys. 71 (12) (2009) 1267–1276.
[32] P.S. Monks, S. Beirle, Applications of satellite observations of tropospheric composition, in: The Remote Sensing of Tropospheric Composition from Space, Springer, 2011, pp. 365–449.
[33] S.K. Kharol, K. Badarinath, A.R. Sharma, D.V. Mahalakshmi, D. Singh, V.K. Prasad, Black carbon aerosol variations over Patiala city, Punjab, India–a study during agriculture crop residue burning period using ground measurements and satellite data, J. Atmos. Sol. Terr. Phys. 84 (2012) 45–51.
[34] K.P. Vadrevu, K. Lasko, L. Giglio, C. Justice, Analysis of southeast asian pollution episode during june 2013 using satellite remote sensing datasets, Environ. Pollut. 195 (2014) 245–256.
[35] T.T.N. Nguyen, H.Q. Bui, H.V. Pham, H.V. Luu, C.D. Man, H.N. Pham, H.T. Le, T.T. Nguyen, Particulate matter concentration mapping from MODIS satellite data: a vietnamese case study, Environ. Res. Lett. 10 (9) (2015) 095016.
[36] B.N. Holben, T.F. Eck, I. Slutsker, D. Tanre, J.P. Buis, A. Setzer, E. Vermote, J.A. Reagan, Y.J. Kaufman, T. Nakajima, et al., AERONET–A federated instrument network and data archive for aerosol characterization, Remote Sens. Environ. 66 (1) (1998) 1–16.
[37] R.C. Levy, S. Mattoo, L.A. Munchak, L.A. Remer, A.M. Sayer, F. Patadia, N.C. Hsu, The collection 6 MODIS aerosol products over land and ocean, Atmos. Meas. Tech. 6 (11) (2013) 2989.
[38] N.C. Hsu, J. Lee, A.M. Sayer, W. Kim, C. Bettenhausen, S.-C. Tsay, VIIRS deep blue aerosol products over land: extending the EOS long-term aerosol data records, J. Geophys. Res. Atmos. 124 (7) (2019) 4026–4053.
[39] E. Abokyi, P. Appiah-Konadu, F. Abokyi, E.F. Oteng-Abayie, Industrial growth and emissions of CO2 in Ghana: the role of financial development and fossil fuel consumption, Energy Rep. 5 (2019) 1339–1353.
[40] C.P. García-Pando, M.C. Stanton, P.J. Diggle, S. Trzaska, R.L. Miller, J.P. Perlwitz, J.M. Baldasano, E. Cuevas, P. Ceccato, P. Yaka, et al., Soil dust aerosols and wind as predictors of seasonal meningitis incidence in Niger, Environ. Health Perspect. 122 (7) (2014) 679.
[41] M. Stafoggia, S. Zauli-Sajani, J. Pey, E. Samoli, E. Alessandrini, X. Basagaña, A. Cernigliaro, M. Chiusolo, M. Demaria, J. Díaz, et al., Desert dust outbreaks in Southern Europe: contribution to daily PM10 concentrations and short-term associations with mortality and hospital admissions, Environ. Health Perspect. 124 (4) (2016) 413.
[42] C.E. Reeves, P. Formenti, C. Afif, G. Ancellet, J.-L. Attié, J. Bechara, A. Borbon, F. Cairo, H. Coe, S. Crumeyrolle, et al., Chemical and aerosol characterisation of the troposphere over west africa during the monsoon period as part of AMMA, Atmos. Chem. Phys. 10 (16) (2010) 7575–7601.
[43] F. De Longueville, Y.-C. Hountondji, S. Henry, P. Ozer, What do we know about effects of desert dust on air quality and human health in west africa compared to other regions? Sci. Total Environ. 409 (1) (2010) 1–8.
[44] A. Sunnu, G. Afeti, F. Resch, A long-term experimental study of the saharan dust presence in West Africa, Atmos Res 87 (1) (2008) 13–26.
[45] M. Aklesso, K.R. Kumar, L. Bu, R. Boiyo, Analysis of spatial-temporal heterogeneity in remotely sensed aerosol properties observed during 2005–2015 over three countries along the Gulf of Guinea Coast in Southern West Africa, Atmos. Environ. 182 (2018) 313–324.
[46] B. Barry, E. Obuobie, M. Andreini, W. Andah, M. Pluquet, The volta river basin, Comparative Study of River Basin Development and Management. Rapport, IWMI, CAWMA, 2005.
[47] G. Lacombe, M. McCartney, G. Forkuor, Drying climate in Ghana over the period 1960–2005: evidence from the resampling-based Mann-Kendall test at local and regional levels, Hydrol. Sci. J. 57 (8) (2012) 1594–1609.
[48] L.K. Amekudzi, E.I. Yamba, K. Preko, E.O. Asare, J. Aryee, M. Baidu, S.N.A. Codjoe, Variabilities in rainfall onset, cessation and length of rainy season for the various agro-ecological zones of Ghana, Climate 3 (2) (2015) 416–434.
[49] B. Sultan, S. Janicot, The West African monsoon dynamics. Part II: the “preonset” and “onset” of the summer monsoon, J. Clim. 16 (21) (2003) 3407–3427.
[50] J. Aryee, L.K. Amekudzi, E. Quansah, N. Klutse, W.A. Atiah, C. Yorke, Development of high spatial resolution rainfall data for Ghana, Int. J. Climatol. 38 (3) (2018) 1201–1215.
[51] R. Manzanas, L.K. Amekudzi, K. Preko, S. Herrera, J.M. Gutiérrez, Precipitation variability and trends in ghana: an intercomparison of observational and reanalysis products, Clim. Change 124 (4) (2014) 805–819.
[52] M. Baidu, L.K. Amekudzi, J.N.A. Aryee, T. Annor, Assessment of long-term spatio-temporal rainfall variability over ghana using wavelet analysis, Climate 5 (2) (2017) 30.
[53] F.A. Asante, F. Amuakwa-Mensah, Climate change and variability in ghana: stocktaking, Climate 3 (1) (2015) 78–99.
[54] K.W. Agyemang-Bonsu, I.K. Dontwi, D.a. Tutu-Benefoh, D.E. Bentil, O.G. Boateng, K. Asuobonteng, W. Agyemang, Traffic-data driven modelling of vehicular emissions using COPERT III in Ghana: a case study of Kumasi(2010).
[55] R.C. Levy, L.A. Remer, S. Mattoo, E.F. Vermote, Y.J. Kaufman, Second-generation operational algorithm: retrieval of aerosol properties over land from inversion of moderate resolution imaging spectroradiometer spectral reflectance, J. Geophys. Res. Atmos. 112 (D13) (2007).

[56] L.A. Remer, R.G. Kleidman, R.C. Levy, Y.J. Kaufman, D. Tanré, S. Mattoo, J.V. Martins, C. Ichoku, I. Koren, H. Yu, et al., Global aerosol climatology from the MODIS satellite sensors, J. Geophys. Res. Atmos. 113 (D14) (2008).
[57] R.C. Levy, L.A. Remer, R.G. Kleidman, S. Mattoo, C. Ichoku, R. Kahn, T.F. Eck, Global evaluation of the collection 5 MODIS dark-target aerosol products over land, Atmos. Chem. Phys. 10 (21) (2010) 10399–10420.
[58] J. Wei, Z. Li, Y. Peng, L. Sun, Modis collection 6.1 aerosol optical depth products over land and ocean: validation and comparison, Atmos. Environ. 201 (2019) 428–440.
[59] M. Tao, L. Chen, Z. Wang, J. Tao, H. Che, X. Wang, Y. Wang, Comparison and evaluation of the MODIS collection 6 aerosol data in China, J. Geophys. Res. Atmos. 120 (14) (2015) 6992–7005.
[60] L.A. Remer, S. Mattoo, R.C. Levy, L.A. Munchak, Modis 3 km aerosol product: algorithm and global perspective, Atmos Meas Tech 6 (7) (2013) 1829.
[61] S. Mattoo, Aerosol dark target (10km & 3km) collection 6.1 changes, 2017.
[62] X. Tian, Q. Liu, X. Li, J. Wei, Validation and comparison of MODIS C6. 1 and C6 aerosol products over Beijing, China, Remote Sens. 10 (12) (2018) 2021.
[63] W. Xu, W. Wang, L. Wu, New regression method to merge different MODIS aerosol products based on NDVI datasets, Atmosphere 10 (6) (2019) 303.
[64] T.F. Eck, B.N. Holben, J.S. Reid, O. Dubovik, A. Smirnov, N.T. O'neill, I. Slutsker, S. Kinne, Wavelength dependence of the optical depth of biomass burning, urban, and desert dust aerosols, J. Geophys. Res. Atmos. 104 (D24) (1999) 31333–31349.
[65] D.M. Giles, A. Sinyuk, M.G. Sorokin, J.S. Schafer, A. Smirnov, I. Slutsker, T.F. Eck, B.N. Holben, J.R. Lewis, J.R. Campbell, et al., Advancements in the aerosol robotic network (AERONET) version 3 database–automated near-real-time quality control algorithm with improved cloud screening for sun photometer aerosol optical depth (AOD) measurements, Atmos. Meas. Tech. 12 (1) (2019).
[66] P. Gupta, M.N. Khan, A. da Silva, F. Patadia, Modis aerosol optical depth observations over urban areas in pakistan: quantity and quality of the data for air quality monitoring, Atmos. Pollut. Res. 4 (1) (2013) 43–52.
[67] K.R. Kumar, V. Sivakumar, R.R. Reddy, K.R. Gopal, A.J. Adesina, Inferring wavelength dependence of AOD and ångström exponent over a sub-tropical station in south africa using AERONET data: influence of meteorology, long-range transport and curvature effect, Sci. Total Environ. 461 (2013) 397–408.
[68] B. Roy, R. Mathur, A.B. Gilliland, S.C. Howard, A comparison of CMAQ-based aerosol properties with IMPROVE, MODIS, and AERONET data, J. Geophys. Res. Atmos. 112 (D14) (2007).
[69] H. Che, L. Yang, C. Liu, X. Xia, Y. Wang, H. Wang, H. Wang, X. Lu, X. Zhang, Long-term validation of MODIS C6 and C6. 1 dark target aerosol products over China using CARSNET and AERONET, Chemosphere 236 (2019) 124268.
[70] Y. Wang, Q. Yuan, T. Li, H. Shen, L. Zheng, L. Zhang, Large-scale MODIS AOD products recovery: spatial-temporal hybrid fusion considering aerosol variation mitigation, ISPRS J. Photogramm. Remote Sens. 157 (2019) 1–12.
[71] Y. Wang, Q. Yuan, T. Li, H. Shen, L. Zheng, L. Zhang, Evaluation and comparison of MODIS collection 6.1 aerosol optical depth against AERONET over regions in China with multifarious underlying surfaces, Atmos. Environ. 200 (2019) 280–301.
[72] A.M. Sayer, N.C. Hsu, J. Lee, W.V. Kim, S.T. Dutcher, Validation, stability, and consistency of MODIS collection 6.1 and VIIRS version 1 deep blue aerosol data over land, J. Geophys. Res. Atmos. 124 (8) (2019) 4658–4688.
[73] G. Huang, Y. Chen, Z. Li, Q. Liu, Y. Wang, Q. He, T. Liu, X. Liu, Y. Zhang, J. Gao, et al., Validation and accuracy analysis of the collection 6.1 MODIS aerosol optical depth over the westernmost city in china based on the sun-sky radiometer observations from SONET, Earth Space Sci. 7 (3) (2020). e2019EA001041
[74] C.J. Willmott, K. Matsuura, Advantages of the mean absolute error (MAE) over the root mean square error (RMSE) in assessing average model performance, Clim. Res. 30 (1) (2005) 79–82.
[75] M. Filonchyk, V. Hurynovich, Validation of MODIS aerosol products with AERONET measurements of different land cover types in areas over Eastern Europe and China, J. Geovisualization Spatial Anal. 4 (2020) 1–11.
[76] R.C. Levy, S. Mattoo, V. Sawyer, Y. Shi, P.R. Colarco, A.I. Lyapustin, Y. Wang, L.A. Remer, Exploring systematic offsets between aerosol products from the two MODIS sensors, Atmos Meas. Tech. 11 (7) (2018) 4073–4092.
[77] R.J. Charlson, S.E. Schwartz, J.M. Hales, R.D. Cess, J.J.A. Coakley, J.E. Hansen, D.J. Hofmann, Climate forcing by anthropogenic aerosols, Science 255 (5043) (1992) 423–430.
[78] M.L. Carroll, C.M. DiMiceli, J. Townshend, R.A. Sohlberg, A.I. Elders, S. Devadiga, A.M. Sayer, R.C. Levy, Development of an operational land water mask for MODIS collection 6, and influence on downstream data products, Int. J. Digital Earth 10 (2) (2017) 207–218.
[79] U.-G. V. Project, Volta basin transboundary diagnostic analysis(2012).
[80] E.W. Hewson, L.E. Olsson, Lake effects on air pollution dispersion, J. Air Pollut. Control Assoc. 17 (11) (1967) 757–761.
[81] Q. Xie, Q. Sun, Monitoring the spatial variation of aerosol optical depth and its correlation with land use/land cover in Wuhan, China: aperspective of urban planning, Int. J. Environ. Res. Public Health 18 (3) (2021) 1132.
[82] M. Kalapureddy, P. Devara, Pre-monsoon aerosol optical properties and spatial distribution over the arabian sea during 2006, Atmos Res. 95 (2–3) (2010) 186–196.
[83] E. Alonso-Blanco, A.I. Calvo, V. Pont, M. Mallet, R. Fraile, A. Castro, Impact of biomass burning on aerosol size distribution, aerosol optical properties and associated radiative forcing, Aerosol. Air Qual. Res. 14 (2014) 708–724.
[84] P. Knippertz, A.H. Fink, R. Schuster, J. Trentmann, J.M. Schrage, C. Yorke, Ultra-low clouds over the southern west african monsoon region, Geophys. Res. Lett. 38 (21) (2011).
[85] R. van der Linden, A.H. Fink, R. Redl, Satellite-based climatology of low-level continental clouds in southern west africa during the summer monsoon season, J. Geophys. Res. Atmos. 120 (3) (2015) 1186–1201.
[86] J. Huang, N.C. Hsu, S.-C. Tsay, M.-J. Jeong, B.N. Holben, T.A. Berkoff, E.J. Welton, Susceptibility of aerosol optical thickness retrievals to thin cirrus contamination during the BASE-ASIA campaign, J. Geophys. Res. Atmos. 116 (D8) (2011).
[87] P. Gupta, L.A. Remer, R.C. Levy, S. Mattoo, Validation of MODIS 3 km land aerosol optical depth from NASA's EOS terra and aqua missions, Atmos Meas. Tech. 11 (5) (2018) 3145–3159.
[88] P. Gupta, L.A. Remer, F. Patadia, R.C. Levy, S.A. Christopher, High-resolution gridded level 3 aerosol optical depth data from MODIS, Remote Sens. 12 (17) (2020) 2847.
[89] R.R. Draxler, G.D. Rolph, HYSPLIT (Hybrid single-particle lagrangian integrated trajectory) model access via NOAA ARL READY. NOAA air resources laboratory, silver spring, md, Dostupno na: http://ready.arl.noaa.gov/HYSPLIT.php (06. 06. 2010.) (2003).
[90] C.D. O'Dowd, M.H. Smith, I.E. Consterdine, J.A. Lowe, Marine aerosol, sea-salt, and the marine sulphur cycle: a short review, Atmos. Environ. 31 (1) (1997) 73–80.
[91] G. De Leeuw, E.L. Andreas, M.D. Anguelova, C.W. Fairall, E.R. Lewis, C. O'Dowd, M. Schulz, S.E. Schwartz, Production flux of sea spray aerosol, Rev. Geophys. 49 (2) (2011).
[92] R.J. Charlson, J.E. Lovelock, M.O. Andreae, S.G. Warren, Oceanic phytoplankton, atmospheric sulphur, cloud albedo and climate, Nature 326 (6114) (1987) 655.